ISSN 1674-1056
http://cpb.iphy.ac.cn
http://iopscience.iop.org/cpb
中国物理 B
Chinese Physics
中国物理
Chinese Physics B

A new cellular automaton model accounting for stochasticity in traffic flow induced by heterogeneity in driving behavior

Xiaoyong Ni(倪晓勇), Hong Huang(黄弘)
Citation: Chin. Phys. B . 2019, 28(9): 098901 . **doi:** 10.1088/1674-1056/28/9/098901
Journal homepage: http://cpb.iphy.ac.cn; http://iopscience.iop.org/cpb

What follows is a list of articles you may be interested in

Evacuation flow of pedestrians considering compassion effect

Yu-Zhang Chen(陈煜章), Ming Li(李明), Rui Jiang(姜锐), Mao-Bin Hu(胡茂彬)
Chin. Phys. B . 2018, 27(8): 088901 . **doi:** 10.1088/1674-1056/27/8/088901

Analysis of dynamic features in intersecting pedestrian flows

Hai-Rong Dong(董海荣), Qi Meng(孟琦), Xiu-Ming Yao(姚秀明), Xiao-Xia Yang(杨晓霞), Qian-Ling Wang(王千龄)
Chin. Phys. B . 2017, 26(9): 098902 . **doi:** 10.1088/1674-1056/26/9/098902

Bottleneck effects on the bidirectional crowd dynamics

Xiao-Xia Yang(杨晓霞), Hai-Rong Dong(董海荣), Xiu-Ming Yao(姚秀明), Xu-Bin Sun(孙绪彬)
Chin. Phys. B . 2016, 25(12): 128901 . **doi:** 10.1088/1674-1056/25/12/128901

Pedestrian choice behavior analysis and simulation of vertical walking facilities in transfer station

Yong-Xing Li(李永行), Hong-Fei Jia(贾洪飞), Jun Li(李军), Ya-Nan Zhou(周亚楠), Zhi-Lu Yuan(原志路), Yan-Zhong Li(李延忠)
Chin. Phys. B . 2016, 25(10): 108901 . **doi:** 10.1088/1674-1056/25/10/108901

Self-organized phenomena of pedestrian counterflow through a wide bottleneck in a channel

Li-Yun Dong(董力耘), Dong-Kai Lan(蓝冬恺), Xiang Li(李翔)
Chin. Phys. B . 2016, 25(9): 098901 . **doi:** 10.1088/1674-1056/25/9/098901

A new cellular automaton model accounting for stochasticity in traffic flow induced by heterogeneity in driving behavior*

Xiaoyong Ni(倪晓勇)[1,2] and Hong Huang(黄弘)[1,2,†]

[1] Institute of Public Safety Research, Department of Engineering Physics, Tsinghua University, Beijing 100084, China
[2] Beijing Key Laboratory of City Integrated Emergency Response Science, Tsinghua University, Beijing 100084, China

(Received 27 February 2019; revised manuscript received 25 June 2019; published online 23 August 2019)

A new reliable cellular automaon (CA) model designed to account for stochasticity in traffic flow induced by heterogeneity in driving behavior is presented. The proposed model differs from most existing CA models in that this new model focuses on describing traffic phenomena by coding into its rules the key idea that a vehicle's moving state is directly determined by a driver stepping on the accelerator or on the brake (the vehicle's acceleration). Acceleration obeys a deformed continuous distribution function when considering the heterogeneity in driving behavior and the safe distance, rather than equaling a fixed acceleration value with a probability, as is the rule in many existing CA models. Simulation results show that the new proposed model is capable of reproducing empirical findings in real traffic system. Moreover, this new model makes it possible to implement in-depth analysis of correlations between a vehicle's state parameters.

Keywords: cellular automaton, numerical simulations, traffic models

PACS: 89.40.–a, 45.70.Vn, 07.05.Tp **DOI:** 10.1088/1674-1056/ab343b

1. Introduction

To investigate dynamic traffic flow behavior on road segments in heavily populated cities, and to obtain a clear understanding of traffic phenomena, a number of models have been proposed. These models can be classified into macroscopic, mesoscopic, and microscopic models according to different scales of stepping mechanism. Macroscopic models, which mainly include fluid-dynamics models[1] and gas-kinetic-based models,[2] describe traffic in aggregated quantities. Microscopic models, which mainly include car-following models[3] and cellular automaton models,[4] focus on describing the status of each vehicle. At the intersection between macroscopic and microscopic models, the mesoscopic modelling applies principles of non-equilibrium statistical mechanics to kinetic theory to model the traffic flow.[5] For details on available traffic simulation methods and tools which can be used at various modelling levels, the reader can redirect to the work of Barceló.[6]

Cellular automaton (CA) model in traffic flow simulation was first proposed by Nagel and Schreckenberg in 1992. Four step updating rules were developed in NaSch model including acceleration, deceleration, random delay, and position update which laid a good foundation for reproducing the phenomenon of real traffic flow.[7] The classic NaSch model is however, limited in that it cannot reproduce some essential features of traffic flow such as phase separation and the hysteresis effect, *etc*.[8,9] Kerner therefore proposed a three-phase theory of traffic,[10] which divides congested traffic into two phases: synchronized flow and wide moving jams. Many models based on Kerner's theory followed,[11–16] and were able to successfully reproduce the fundamental diagram of traffic and the spatiotemporal shapes of the different traffic phases. Moreover, there are many studies on traffic flow behavior in different scenarios based on CA models,[17–22] which all prove that CA models are able to provide considerable insight into traffic behavior and are very promising alternatives to modeling traffic flow and understanding its behavior despite that different models usually have different advantages and disadvantages.[23]

The biggest common advantage of CA models is local rule-based mechanism, which means that vehicles make decisions based on their goals, their current situation, and interactions with their surroundings. This peculiarity ensures that CA models are able to capture micro-level dynamics.[24] However, there is a disadvantage of CA models in micro-level step updating mechanism which received little attention in the last decades when we look into models' micro-level dynamics. Most existing CA models include the rule that vehicles adjust their velocity directly according to the headway distance and take into consideration the stochasticity in traffic flow by introducing a certain probability in control of changes in vehicles' velocity.[25–27] Consequently, vehicles tend to change speed abruptly, exceeding the real vehicular acceleration/deceleration capabilities and producing erratic acceleration/deceleration behavior.[28] Some CA models introduce limited acceleration/deceleration capability into the

*Project supported by the National Key Research and Development Program of China (Grant No. 2018YFC0809900) and the National Natural Science Foundation of China (Grant Nos. 71774093 and 71473146).

†Corresponding author. E-mail: hhong@tsinghua.edu.cn

© 2019 Chinese Physical Society and IOP Publishing Ltd

CA traffic flow model[29] and set the acceleration and deceleration rates to be specific constants with a certain probability according to the traffic condition. This setting is able to overcome the erratic acceleration/deceleration problem. However, these models are still unrealistic since it is known, from many observed trajectories in real traffic, that different accelerations/decelerations induced by heterogeneity in driving behavior usually are continuously distributed random variables and are highly related to safe distance[30] and relative velocity between adjacent vehicles.[31,32] In brief, despite plentiful research on CA modelling application, insufficient attention has been paid to improving models' fundamental micro-level step updating mechanism coupling with the consideration of safe distance and relative velocity between adjacent vehicles. This motivated the writing of this paper.

In this paper, a new CA model accounting for stochasticity in traffic flow induced by heterogeneity in driving behavior is proposed for traffic flow, which is both simple and reliable. Our model also introduces the concept of safe distances to give a more reasonable upper limit to acceleration of vehicles. The two main new features introduced are: (i) A vehicle's moving state is directly determined by a driver's action of accelerating or braking (acceleration of a vehicle), rather than assuming velocity is directly determined by the headway distance; (ii) The acceleration rate in this model obeys a deformed continuous distribution function according to the annual research report prepared for the U.S. Department of Transportation.[33] These new features make our proposed model more realistic in traffic flow simulation.

The remainder of this paper is organized as follows. Section 2 presents methodology, Section 3 shows the study scenario and Section 4 shows the results and model verification. Finally Section 5 concludes this paper.

2. Methodology

2.1. Basic settings of the new CA model

The new proposed model is defined on a lattice of length L, where each cell can be empty or occupied by just one vehicle. The system consists of N vehicles moving in one direction in a single lane, therefore overtaking and lane changing are not permitted. The speed of each vehicle can take on one of the $(V_{\max}+1)$ allowed integer values $v = 0, 1, \ldots, v_{\max}$. For simplicity, we only consider one type of vehicle in this paper and therefore, the same maximum velocity $v_{\max}$ will be used for all vehicles. $\pm M$ denotes the maximum acceleration rate in quick start (emergency braking). $\pm\mu_{\mathrm{c}}$ denotes the comfortable acceleration (deceleration) rate. t_{s} denotes the time step. $x_n(t)$ and $x_{n+1}(t)$ denote the location of the vehicle n and $n+1$ respectively at time t. $v_n(t)$ and $v_{n+1}(t)$ denote the velocity of the vehicle n and $n+1$ respectively at time t. $a_n(t)$ denotes the acceleration of vehicle n at time t. $d_n(t)$ denotes the actual distance between vehicles n and $n+1$, that is the distance from the front bumper of vehicle n to the rear bumper of vehicle $n+1$. $d_n(t) = x_{n+1}(t) - x_n(t) - l_{\mathrm{vehicle}}$, where l_{vehicle} denotes the vehicle length. It is assumed that the position of a vehicle is denoted by the cell that contains its rear bumper.

2.2. Safety criteria and the distribution function of acceleration in the new CA model

A definition of safe distance d_{safe} is introduced before considering the micro-level step updating mechanism of the model. Suppose there are N vehicles in total, denoted by $1, 2, 3, \ldots, i \ldots, N$. The safe distance between vehicle n and $n+1$, denoted by $d_{\mathrm{safe}_n}(t)$, can be calculated by

$$d_{\mathrm{safe}_n}(t) = \sum_{i=0}^{(v_n(t)+a_n(t))_{\mathrm{div}M}} [v_n(t) + a_n(t) - i \times M] - \sum_{i=0}^{(v_{n+1}(t)-M)_{\mathrm{div}M}} [(v_{n+1}(t) - M) - i \times M], \quad (1)$$

where M is the absolute value of the maximum acceleration of the vehicles. $X_{\mathrm{div}Y}$ is the integer division, meaning that $X_{\mathrm{div}Y} = \lceil X/Y \rceil$, where "/" is normal division, and $\lceil z \rceil$ is the floor function. The value of $\lceil z \rceil$ should be the integer closest to z, but smaller than z. $d_{\mathrm{safe}_n}(t)$ depicts a safe distance in the extreme situation: the preceding vehicle breaks sharply at time t, while the following vehicle accelerates at a rate $a_n(t)$. The following vehicle will become aware of the emergency situation, and brake sharply at time $t+1$. In this situation the first term of the polynomial denotes the distance traveled by the following vehicle while the second term of the polynomial denotes the distance traveled by the preceding vehicle. Thus the difference, $d_{\mathrm{safe}_n}(t)$, denotes the safe distance, which means that these two vehicles must keep at least this distance apart to avoid a collision. Correspondingly, the value of $d_{\mathrm{safe}_n}(t)$ can be recorded as $d_{\mathrm{acc_}M_n}(t)$ when $a_n(t) = +M$, $d_{\mathrm{keep}_n}(t)$ when $a_n(t) = 0$ and $d_{\mathrm{dec_}M_n}(t)$ when $a_n(t) = -M$. Suppose that $b_n(t)$ denotes the solution of the following equation if the solution set exists:

$$d_n(t) = \sum_{i=0}^{(v_n(t)+b_n(t))_{\mathrm{div}M}} [v_n(t) + b_n(t) - i \times M] - \sum_{i=0}^{(v_{n+1}(t)-M)_{\mathrm{div}M}} [(v_{n+1}(t) - M) - i \times M]. \quad (2)$$

Then the interval of the acceleration $A_n(t)$ can be calculated by Eq. (3). The lower limit of the acceleration interval continues to be $-M$ in different situations because it is a common belief that drivers pay more attention to deceleration than to acceleration for safety reasons.[34] It is possible for drivers in real life to maintain a constant velocity or to decelerate even

when acceleration is allowed due to the heterogeneity in driving behavior

$$A_n(t)=\begin{cases}[-M,+M], & \text{if } d_n(t)\geqslant d_{\text{acc_}Mn}(t),\\ [-M,b_n(t)], & \text{if } d_{\text{keep}_n}(t)\leqslant d_n(t)<d_{\text{acc_}Mn}(t),\\ [-M,b_n(t)], & \text{if } d_{\text{dec_}Mn}(t)<d_n(t)<d_{\text{keep}_n}(t),\\ \{-M\}, & \text{if } d_n(t)\leqslant d_{\text{dec_}Mn}(t).\end{cases} \tag{3}$$

Here $b_n(t)>0$ if $d_{\text{keep}_n}(t)\leqslant d_n(t)<d_{\text{acc_}M_n}(t)$ while $b_n(t)<0$ if $d_{\text{dec_}M_n}(t)\leqslant d_n(t)<d_{\text{keep}_n}(t)$.

According to many previous studies, if a driver decides to accelerate or decelerate they prefer to use the comfortable acceleration $\pm\mu_c$.[28] However, there is also a possibility that the rate of acceleration will deviate $\pm\mu_c$. Considering that a Gaussian distribution describes the distribution of the acceleration well,[33] a deformed Gaussian distribution is introduced to describe the distribution of the acceleration because the upper limit (lower limit) of the acceleration distribution is a specific integer value in our CA model, instead of positive infinity (negative infinity) in normal Gaussian distribution functions.

If $X\sim N(\mu,\sigma^2)$, the distribution function for the random variable X is

$$F_s(x)=\frac{1}{\sqrt{2\pi}\sigma}\int_{-\infty}^{x}\exp\left[-\frac{(t-\mu)^2}{2\sigma^2}\right]\mathrm{d}t. \tag{4}$$

The probability density function of the acceleration proposed in this paper is

$$f(a_n(t))=\begin{cases}\dfrac{1}{F_s(M)-F_s(-M)}\dfrac{1}{\sqrt{2\pi}\sigma}\exp\left[-\dfrac{(a_n(t)-\mu_c)^2}{2\sigma^2}\right], & a_n(t)\in[-M,M], \quad \text{if } d_n(t)\geq d_{\text{acc_}M_n}(t),\\ \dfrac{1}{F_s(b_n(t))-F_s(-M)}\dfrac{1}{\sqrt{2\pi}\sigma}\exp\left[-\dfrac{(a_n(t)-\mu_c)^2}{2\sigma^2}\right], & a_n(t)\in[-M,b_n(t)],\ \text{if } d_{\text{keep}_n}(t)\leq d_n(t)<d_{\text{acc_}M_n}(t),\\ \dfrac{1}{F_s(b_n(t))-F_s(-M)}\dfrac{1}{\sqrt{2\pi}\sigma}\exp\left[-\dfrac{(a_n(t)+\mu_c)^2}{2\sigma^2}\right], & a_n(t)\in[-M,b_n(t)],\ \text{if } d_{\text{dec_}M_n}(t)<d_n(t)<d_{\text{keep}_n}(t).\end{cases} \tag{5}$$

In the above equation, the terms $1/(F_s(M)-F_s(-M))$ and $1/(F_s(b_n(t))-F_s(-M))$ are constant adjustment terms to ensure that the integral of the probability density function for a specified interval equals one. When $d_n(t)\geqslant d_{\text{keep}_n}(t)$, the mathematical expectation of the distribution is $+\mu_c$, which illustrates that the vehicle tends to accelerate at a comfortable rate. Of course, there is a small possibility that the vehicle will decelerate, since some drivers do not like to accelerate even if the gap between his/her vehicle and the preceding vehicle is large enough. When $d_n(t)<d_{\text{keep}_n}(t)$, the mathematical expectation of the distribution is $-\mu_c$, which illustrates that the vehicle tends to decelerate at a comfortable rate. The vehicle is not permitted to accelerate in this situation to avoid collision.

The value of acceleration should be a discrete integer in CA models. Thus, the probability of acceleration, $P(a_n(t))$, can be calculated by Eq. (6). Suppose that the upper limit (lower limit) of the interval of acceleration is Limit_u (Limit_l). From the above analysis we can see that $\text{Limit}_u=M$ or $b_n(t)$ while $\text{Limit}_l=-M$. Suppose that X is an integer in the interval $[\text{Limit}_l,\text{Limit}_u]$.

$$P(a_n(t)=X)=\begin{cases}\displaystyle\int_{\max(X-0.5,\text{Limit}_l)}^{\min(X+0.5,\text{Limit}_u)} f(a_n(t))d(a_n(t)), & \text{here } X\in[\text{Limit}_l,\text{Limit}_u], \quad \text{if } d_n(t)>d_{\text{dec_}M_n}(t),\\ 1, & \text{here } X=-M, \quad \text{if } d_n(t)\leqslant d_{\text{dec_}M_n}(t).\end{cases} \tag{6}$$

2.3. Updating rules of the new CA model

One update of the system consists of the following consecutive steps.

Step 1 Calculate the interval of acceleration $A_n(t)$. In this step, we should obtain the values of $d_{\text{acc_}M_n}(t)$, $d_{\text{keep}_n}(t)$, and $d_{\text{dec_}M_n}(t)$. Determine $A_n(t)$ by comparing the value of $d_n(t)$ with $d_{\text{acc_}M_n}(t)$, $d_{\text{keep}_n}(t)$, and $d_{\text{dec_}M_n}(t)$.

Step 2 Determine the acceleration of each vehicle $a_n(t)$. First, we calculate the probability density function of the acceleration $f(a_n(t))$ and then determine the acceleration of each vehicle according to the probability of acceleration $P(a_n(t)=X)$.

Step 3 Change the velocity of vehicles by calculating $v_{n+1}(t)$,

$$v_n(t+1)=\begin{cases}0, & \text{if } v_n(t)+a_n(t)<0,\\ v_n(t)+a_n(t), & \text{if } 0\leqslant v_n(t)+a_n(t)<v_{\max},\\ v_{\max}, & \text{if } v_n(t)+a_n(t)\geqslant v_{\max}.\end{cases} \tag{7}$$

Step 4 Realize vehicle movement. Each vehicle moves forward using its new velocity determined in Step 3:

$$x_n(t+1)\to x_n(t)+v_n(t+1). \tag{8}$$

Here $x_n(t)$ and $v_n(t)$ respectively denote the position and velocity of vehicle n at time step t (it is assumed that vehicle $n+1$ precedes vehicle n).

3. Simulation scenario

The simulation scenario used for the simulation study is described below. We assume that private cars are the only vehicle type for the simulation. According to a previous study, it is plausible to assume that these moving vehicles occupy 5×5 cells if the size of one cell is 1 m×0.5 m.[35] The time step should be set to a driver's reaction time such that after a preceding vehicle brakes sharply, the following vehicle will react by also breaking sharply at the next step. We used a time step t_s of one second, which is an average person's reaction time.[36] Here the model is defined on a lattice of length $L = 10^3$ m $= 10^3$ cells. This simulation scenario is shown in Fig. 1.

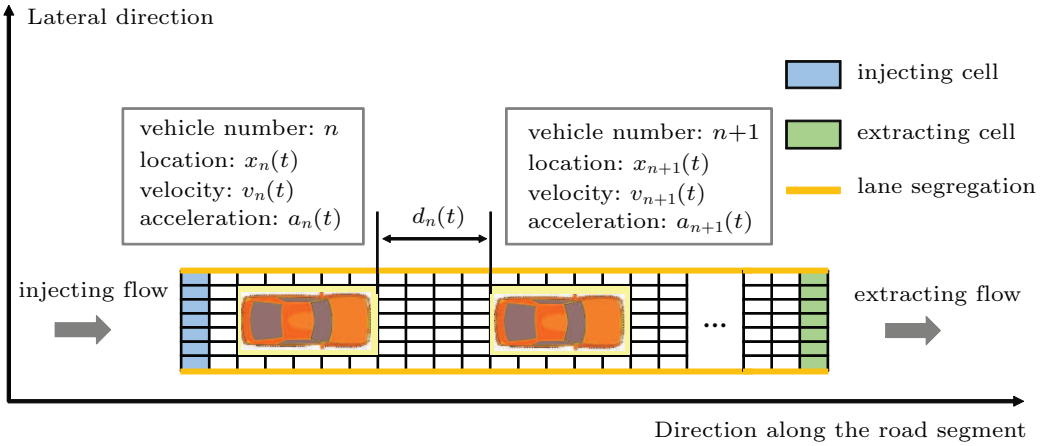


Fig. 1. The simulation scenario in this study.

The speed limit on urban roads in China is 70.00 km/h when there is only one lane in each direction. For this study, the maximum velocity is set to be $v_{\max} = 90.00$ km/h $= 25.00$ m/s $= 25.00$ cells/s, considering that the speed limits of some urban highways are usually a little higher than 70.00 km/h. The maximum acceleration $\pm M$ in quick start (emergency braking) is set to be $M(-M) = 5.00\ \text{m/s}^2(-5.00\ \text{m/s}^2) = 5.00\ \text{cells/s}^2(-5.00\ \text{cells/s}^2)$.[37] Suppose that $a_n(t) \sim N(\mu_c, \sigma^2)$, then σ is set to be 1.00 m/s^2 as a case study. σ represents the significant degree of deviation in the distribution and can be easily modified if necessary. The comfortable acceleration (deceleration) $\pm\mu_c$ is set to be $\mu_c(-\mu_c) = 2.50\ \text{m/s}^2(-2.50\ \text{m/s}^2) = 2.50\ \text{cells/s}^2(-2.50\ \text{cells/s}^2)$ in this study.[28]

4. Results

4.1. Feature diagrams of the system with periodic boundary conditions

Simulation results for a single-lane road segment with periodic boundary conditions are shown here. The injecting cells and the extracting cells are coincident in the periodic boundary conditions. The global density ρ is defined as

$$\rho = N/L. \tag{9}$$

N denotes the number of vehicles involved in this system. A virtual monitoring probe is positioned at the row of the extracting cells. The time-averaged flow q is defined as

$$q = \frac{1}{T}\sum_{t_0+1}^{t_0+T} n_p(t). \tag{10}$$

Here $n_p(t) = 1$ if a vehicle's rear bumper arrives at the extracting cell row and the vehicle's velocity is not zero. This ensures that the vehicle (veh) will only be counted once, even if it is in the extracting cell row for continuous time steps.

Initially, the vehicles stop near the injecting cells in a line and then start up one by one based on the proposed model. In order to get to a stable state of the system, each simulation, with different values for density ρ, is conducted for 3.6×10^3 time steps after a spin-up period of the first 10^3 time steps. Flow, velocity, and density are the commonly used parameters which represent the most important macroscopic traffic characteristics.[38] If the flow is measured in "vehicles/h", the relationship between density ρ and flow q, and the correlation between vehicles' average velocity and density ρ are shown in Fig. 2.

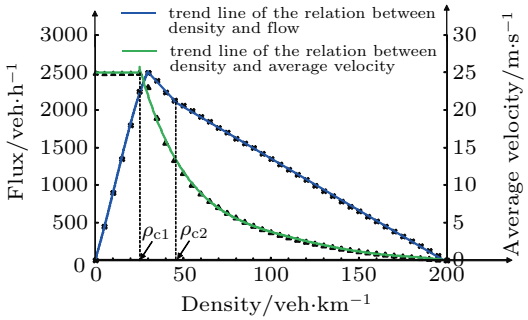


Fig. 2. The fundamental diagram and the correlation between density and velocity of the proposed model.

The density–flow relationship and the density–velocity relationship obtained from the simulations of this model are consistent with the classical and empirical findings obtained in some other prevalent models such as the BJH model,[37]

the Slow-to-start model,[39] and the comfortable driving (CD) model.[40] Our proposed model is also able to reproduce the hysteresis phenomenon and the three phases (free flow, synchronized flow, and jammed flow) observed in real traffic, as is shown in Fig. 2. When the density $\rho < \rho_{c1}$, the traffic flow is in free-flow mode. The critical density $\rho_{c1} \cong 25$ veh/km, which is consistent with various findings in the real world (~ 25 (1/km)).[41] When $\rho_{c1} < \rho < \rho_{c2}$, phase separation is observed, and the traffic flow comprises free flow and congested flow at the same time. As is well known, congested flow includes synchronized flow and jammed flow. When $\rho > \rho_{c2}$, free flow disappears and traffic flow is congested.

The spatiotemporal shapes of different traffic phases (free flow, synchronized flow, and jammed flow) for different simulation scenarios are depicted in Fig. 3. In these scenarios, the density ρ increases from 20 vehicles/km to 180 vehicles/km, in steps of 20 vehicles/km.

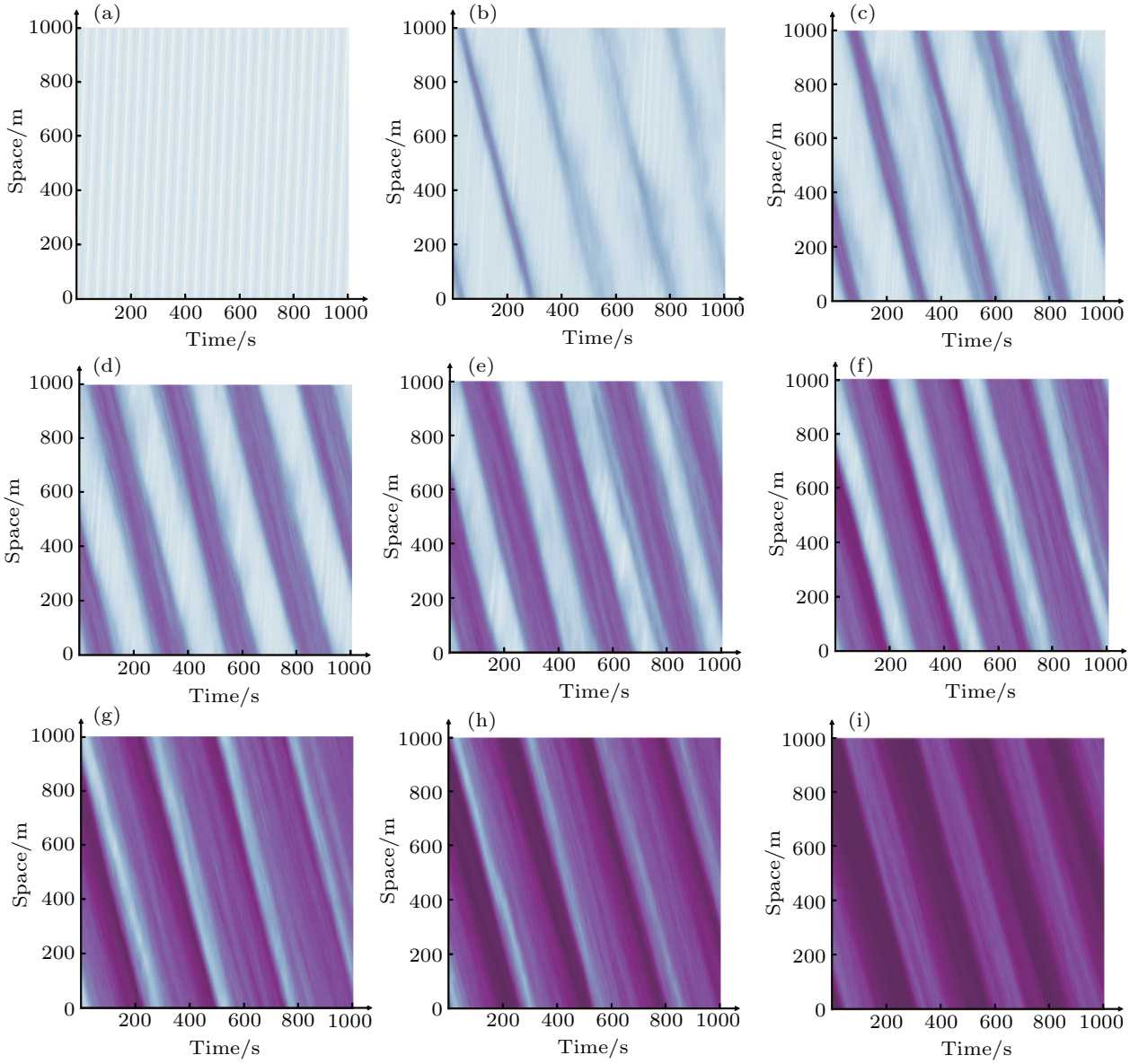


Fig. 3. The spatiotemporal shapes of different traffic phases in different densities: (a) 20 veh/km, (b) 40 veh/km, (c) 60 veh/km, (d) 80 veh/km, (e) 100 veh/km, (f) 120 veh/km, (g) 140 veh/km, (h) 160 veh/km, and (i) 180 veh/km.

From Fig. 3, we see that the traffic flow shown in panel (a) is free, where the flux can be increased along with an increase in car density ρ. In free flow, the space–time trajectories corresponding to different vehicles moving forward can be easily found. Figure 3(b)–figure 3(i) show congested traffic flow with jams moving backwards. With increasing densities, jammed flow gradually pushes out synchronized flow.

To depict the three traffic states (free flow, synchronized flow, and jammed flow) more clearly, figure 4 describes the one minute average flux against the density of the proposed model under periodic boundary conditions. The simulation data are obtained by a virtual probe. This virtual probe can record the flux and velocity of the vehicles which pass through a vertical section perpendicular to the road. We record the flux

q_{local} and average velocity $\bar{v}_{\text{local}}$ using the virtual probe and then calculate the value of the local density by

$$\rho_{\text{local}} = q_{\text{local}}/\bar{v}_{\text{local}}. \tag{11}$$

The most important difference between Fig. 2 and Fig. 4 is that figure 2 describes overall traffic conditions using data points of average values in one hour, while figure 4 describes the local traffic conditions based on the simulation results in one minute. It means that data points in Fig. 4 only represent the situation of one phase or two consecutive phases for the traffic flow has only moved a short distance. Therefore, figure 4 can discern between the different traffic phases (free flow, synchronized flow, and jammed flow) more clearly. The upper scatter boundary with an average velocity of 90 km/h represents the free-flow mode while the lower scatter boundary with an average velocity of 3.6 km/h forms the split between synchronized flow, and jammed flow. Figure 4 shows that the new proposed model can simulate free flow, light synchronized flow (where the average velocity of vehicles is close to the free-flow velocity), and heavy synchronized flow at the same time. As we know, vehicle velocity can vary greatly in real traffic flow in cities. Vehicles can advance at maximum velocity when traffic flow is sparse, but can be stopped for periods of time in jammed traffic. Thus the field of application of the model needs to be broad enough so as to be capable of simulating all the scenarios of real traffic flow. In this respect, the performance of our proposed model is superior to some of the prevalent models such as CD and MCD models.[40,42] In CD model, the average velocity of the upper scatter boundary is 60 km/h which means that the model is not suitable for light synchronized flow simulation. While in MCD model, the average velocity of the lower scatter boundary is 24 km/h which means the model is not suitable for heavy synchronized flow simulation.

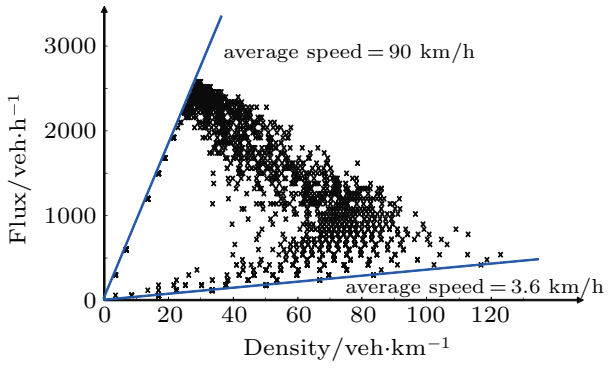


Fig. 4. One minute average flux against density.

4.2. The correlations between a single vehicle's state parameters

We also find that the performance of this proposed model is more realistic by analyzing the correlations between one vehicle's different state parameters. A series correlation analysis of a vehicle's state parameters was conducted to illustrate the performance of the proposed model in a more detailed way.

The distributions of the velocity with different headway distances are shown in Fig. 5. When the headway distance is 5 m, the distribution of the velocity is asymmetrical with a small proportion of vehicular velocities exceeding 5 m/s. The highest velocity in this distribution is 10 m/s, which is considerable since the maximum acceleration in this study is set to be $M\,(-M) = 5.00\ \text{m/s}^2(-5.00\ \text{m/s}^2)$. The velocity changes before the location, so the vehicle with a velocity of 10 m/s will move forward with a velocity of 5 m/s only if its acceleration is $-5\ \text{m/s}^2$. The velocity will decrease to 0 m/s as long as it maintains that acceleration ($-5\ \text{m/s}^2$). In other words, this vehicle will theoretically only move forward 5 m when using the rules in the proposed model, and a potential collision would be avoided under this assumption. Distributions of the velocity with other headway distances can be similarly understood.

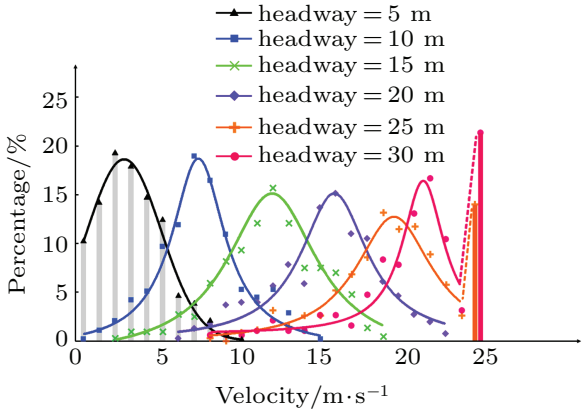


Fig. 5. The distribution of velocity with different headway distances.

The distribution becomes approximately symmetrical and the axis of symmetry moves gradually in the positive direction along the "velocity" axis, together with headway distance increasing (headway = 10 m, 15 m, 20 m). When the headway distance is 25 m or 30 m, the velocity distributions become asymmetrical again and present distributions with two peaks. The second peak is at "velocity = 25 m/s". The second peak becomes bigger with increasing headway distances which means that with a bigger headway distance, more vehicles can move ahead with maximum velocity.

We use nonlinear curve fitting in OriginPro 9.1 to fit the obtained data scatter points. In general, the distribution curves (without the second peak if it exists) fit a Lorentz distribution well in a discrete state with the following probability density function

$$P(v) = p_0 + \left(\frac{2\varphi}{\pi}\right)\cdot\left(\frac{w}{4\,(v-v_{\text{c}})^2 + w^2}\right). \tag{12}$$

The values and standard errors of the parameters, and the R-square values of the equations are listed in Table 1.

Table 1. The values and standard errors of the parameters in Eq. (12).

Headway/m	5	10	15	20	25	30
p_0 value	-3.55×10^{-2}	-9.81×10^{-4}	-1.59×10^{-2}	3.83×10^{-3}	3.39×10^{-3}	8.22×10^{-3}
Standard error	1.48×10^{-2}	7.07×10^{-3}	1.08×10^{-2}	8.88×10^{-3}	5.76×10^{-3}	5.42×10^{-3}
v_c value	2.53	7.27	11.9	16.0	19.8	21.6
Standard error	0.118	0.101	0.173	0.188	0.143	0.135
w value	6.20	4.15	7.04	5.23	5.93	3.27
Standard error	0.747	0.468	1.03	0.908	0.676	0.510
φ value	2.21	1.21	1.70	1.14	1.23	0.797
Standard error	0.354	0.145	0.313	0.218	0.155	0.110
R^2 value	0.972	0.959	0.930	0.896	0.952	0.915

From Table 1 we find that v_c and headway distance have a strong positive correlation. v_c increases along with an increase in the headway distance d. This correlation can be represented with the following equation, where d denotes the headway distance

$$v_c = 38.6 - 42.4 \times e^{-0.0313\cdot d}. \tag{13}$$

Despite knowing that the average velocity increases with an increase in headway distance, whether the model can simulate details of real traffic flow is worth further exploration. We first study the correlation between headway distance and average velocity, with the simulation results grouped according to the difference in velocity between adjacent vehicles. The corresponding results are shown in Fig. 6(a). These results show that the average velocity generally increases with an increase in headway distance, which is in accordance with the results shown in Fig. 5. When the headway distance is less than h_{a1}, the average velocity keeps increasing along with the increase in headway distance. In this process, the average velocity of vehicles is greater if the velocity difference between the vehicle and the vehicle in front is greater. It is easy to understand that the distribution of the velocity is certain when the value of the headway distance is known. Therefore, the mean value of the velocity can be determined. If a following vehicle's velocity is greater than the vehicle in front, that following vehicle's velocity has a higher possibility of being relatively greater. When the headway distance is larger than h_{a1} but smaller than h_{a2}, the average velocity tends towards 25 m/s. With an increase in headway distance, the percentage of the velocity equaling 25 m/s is higher. When the headway distance is larger than h_{a2}, the distribution of the average velocity is almost determined. If the velocity difference is a positive value, the average velocity concentrates at approximately 25 m/s. If the velocity difference is a negative value, the average velocity concentrates at a value less than 25 m/s. The mean values of the average velocities are relatively stable at a certain headway distance which demonstrates that the proposed model performs well and stably when depicting the correlation between the headway distance and average velocity.

We next study the correlation between the headway distance and the average velocity with the simulation results grouped according to the acceleration of vehicles. The corresponding results are shown in Fig. 6(b). These results show that the acceleration is greater when the average velocity is relatively slower for a certain headway distance. This is in accordance with reality since in the same environmental condition, slower vehicles generally have greater motivation to accelerate, to both save themselves some time and because of interactions with adjacent cars. For example, the horn of a rear vehicle will promote the acceleration of the front vehicle. The results show that this proposed model performs reasonably and is in general realistic.

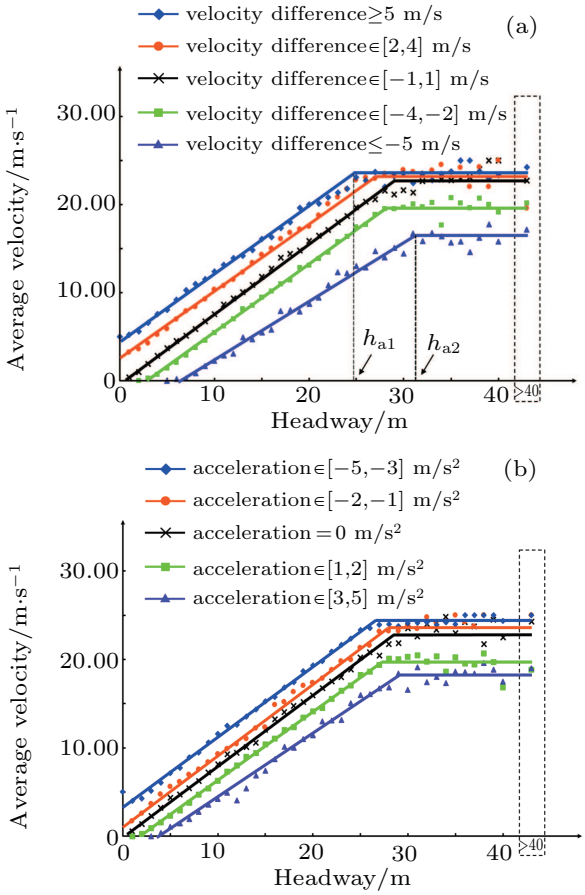


Fig. 6. The correlation between the headway distance in front of a vehicle and the average velocity of that vehicle.

From Fig. 6, it can be seen that when the headway distance is known, the value of the average velocity will be slower if the velocity difference is smaller or the acceleration is greater. It seems that a relatively greater (lesser) acceleration and a relatively lesser (greater) velocity difference both correspond to the same average velocity. Furthermore, we notice that previous studies have found that the effect of velocity difference on acceleration is significant from different field observation data and experiments.[43] For this reason, we looked at the detailed correlation between velocity difference and acceleration. Considering the coupling effect of a vehicle's state parameters, including the velocity difference, headway distance, and velocity, we first constructed a set of state parameter groups to present the possible discrete values of headway distance and velocity for a certain velocity difference. We then calculate the acceleration for this velocity difference using a weighted algorithm. The weighting factor is the probability of an occurrence of each state parameter group in the simulation.

Suppose that $\Delta v(n)$ denotes the velocity difference of vehicle n and vehicle $n+1$; $d(n)$ denotes the headway distance of vehicle n to vehicle $n+1$; $v(n)$ denotes the velocity of vehicle n; $a(n)$ denotes the acceleration of vehicle n. A state parameter group $G_{\Delta v,d,v,a}$ is defined as $G_{\Delta v,d,v,a} = \{\Delta v(k), d(k), v(k), a(k)\}_{k\in\{1,2,\ldots,N\}}$. The number of times that $G_{\Delta v,d,v,a}$ has appeared in the simulation is denoted by $M_{\Delta v,d,v,a}$. Thus, $G_{\Delta v,i,j,a}$ denotes a state parameter group where $d(n) = i$, $(n = 1,2,\ldots,N)$ and $v(n) = j$, $(n = 1,2,\ldots,N)$. It is important to note that $d(n)$ and $v(n)$ are both related to $\Delta v(n)$, here $n = 1,2,\ldots,N$. Therefore, the possible values of i and j are both related to $\Delta v(n)$ $(n = 1,2,\ldots,N)$. Suppose that $I_{u\Delta v}$ ($I_{l\Delta v}$) and $J_{u\Delta v}$ ($J_{l\Delta v}$) denote the maximum (minimum) of the set of i and j. $P_{\Delta v,i,j,a}$ denotes the probability of the occurrence of $G_{\Delta v,i,j,a}$,

$$P_{\Delta v,i,j,a} = M_{\Delta v,i,j,a} \Big/ \sum_{J_{l\Delta v}}^{J_{u\Delta v}} \left(\sum_{I_{l\Delta v}}^{I_{u\Delta v}} M_{\Delta v,i,j,a} \right). \tag{14}$$

Therefore, it is apparent that

$$\begin{aligned} P_{\Delta v,a} &= \sum_{J_{l\Delta v}}^{J_{u\Delta v}} \left(\sum_{I_{l\Delta v}}^{I_{u\Delta v}} P_{\Delta v,i,j,a} \right) \\ &= \sum_{J_{l\Delta v}}^{J_{u\Delta v}} \sum_{I_{l\Delta v}}^{I_{u\Delta v}} M_{\Delta v,i,j,a} \Big/ \sum_{J_{l\Delta v}}^{J_{u\Delta v}} \left(\sum_{I_{l\Delta v}}^{I_{u\Delta v}} M_{\Delta v,i,j,a} \right) \\ &= 1. \end{aligned} \tag{15}$$

Returning to the study of the correlation between the velocity difference and acceleration, the mean and standard deviation of the acceleration are defined by the following equations:

$$\bar{a}_{\Delta v} = \sum_{J_{l\Delta v}}^{J_{u\Delta v}} \left(\sum_{I_{l\Delta v}}^{I_{u\Delta v}} a \cdot P_{\Delta v,i,j,a} \right), \tag{16}$$

$$S(a_{\Delta v}) = \sqrt{\sum_{J_{l\Delta v}}^{J_{u\Delta v}} \left(\sum_{I_{l\Delta v}}^{I_{u\Delta v}} (a - \bar{a}_{\Delta v})^2 \cdot P_{\Delta v,i,j,a} \right)}. \tag{17}$$

The detailed correlation between velocity difference and acceleration is shown in Fig. 7. The mean value of acceleration is $\bar{a}_{\Delta v}$ and the value of the positive and negative error bar is $S(a_{\Delta v})$. When the velocity difference is negative with a large absolute value, the mean of acceleration is around 2.5 m/s^2, which means that most vehicles with a velocity much lower than the vehicle in front of them tend to accelerate at a comfortable rate. This is determined by the rules in the proposed model. With an increase in velocity difference, acceleration reduces gradually from being positive to being negative. When the velocity difference is positive with a large absolute value, the mean of the acceleration is between -4 m/s^2 and -5 m/s^2, instead of -2.5 m/s^2. The absolute value of the mean of the acceleration is less than a comfortable acceleration mainly because of the possibility of needing to brake urgently if the distance between two adjacent vehicles is too small, or the possibility that the vehicle decelerates for any reason, even where acceleration is permitted.

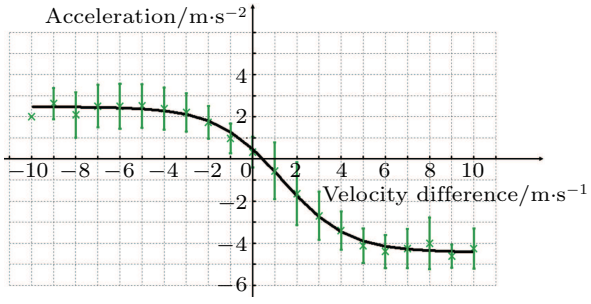


Fig. 7. The correlation between velocity difference and acceleration of vehicles.

The fitting equation in Fig. 7 is shown in the following:

$$a_{\Delta v} = -4.43 + \frac{6.84}{1 + \mathrm{e}^{(\Delta v - 1.32)/1.49}}, \quad R^2 = 0.994. \tag{18}$$

4.3. Model verification

We use data extracted from real traffic flow by other researchers to verify our proposed model from both macroscopic and microscopic perspectives, as shown in Table 2. The data are a type of single-vehicle processed data obtained using Autoscope Rackvision Terra, in which velocities and time-headways of all vehicles passing the equipment can be recorded. Error correction was performed on the data by checking the original videos using Tracker software. The error of every single-vehicle velocity was found to be no more than 1 m/s (3.6 km/h).[44]

Table 2. Two datasets extracted from real traffic flow.

Group	Data type	Flux/(veh/h)	Average velocity by detector/(m/s)	Density/(veh/km)
1	1st real dataset	1780	13.1	37.7
2	2nd real dataset	2044	17.0	33.4

The first dataset was derived from empirical video data on the Nanjing Airport Highway.[45] This highway is the main

road connecting Nanjing urban areas with Nanjing Lukou Airport. There were 40 cameras along the 28-km-long highway which has two lanes in each direction. The second dataset was obtained from a large-scale construction project also situated on the Nanjing Airport Highway. Every day one of the two lanes was temporarily closed on a 5–10-km-long section of road. This enabled the collection of empirical single-lane traffic flow data.[46,47] The speed limit in both traffic scenarios was 120 km/h (≅ 33 m/s).

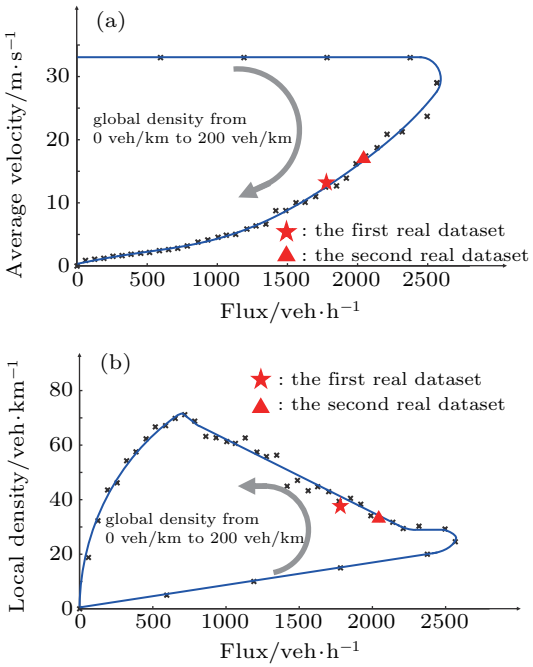


Fig. 8. The comparison of real data sets and the macroscopic performance of the proposed model.

We adjusted the maximum velocity in our proposed model from 25 m/s to 33 m/s to make the simulation conditions same as real traffic scenarios in datasets. A virtual detector was set at the end of the road. Each simulation, using a certain global density lasted for one minute, and sixty groups of simulations with the same global density were conducted. The sum of the fluxes from these sixty groups and the average velocity of the vehicles that passed by the virtual detector were recorded. Then the local densities for different fluxes were calculated using $\rho_{\text{local}} = q_{\text{local}}/\bar{v}_{\text{local}}$. The correlation between average velocity and flux, along with increasing global density in the simulation group is depicted in Fig. 8(a). The correlation between local density and flux along with increasing global density in the simulation group is depicted in Fig. 8(b). The results show that the real data sets are consistent with the macroscopic performance of the proposed model.

The above validation proves that the proposed model is a competitive CA model. The proposed model can simulate traffic flow ensuring the authenticity of the features, and is able to reproduce the empirical findings. Moreover, we found that the acceleration of a vehicle is mostly influenced by the velocity difference when the absolute value of acceleration is not large. This finding is consistent with other studies which showed that acceleration always has a linear correlation to the velocity difference when the absolute value of acceleration is not large.[31,32]

We compare the results produced by our proposed model with those produced by the SVR driving behavior model. Wei and Liu depicted the correlation between relative velocity and acceleration for headway distances of 9 m and 12 m.[31] The relative velocity is in an interval of [–10, 10] km/h ([–2.78, 2.78] m/s). We therefore analyzed the coupled distribution of velocity and velocity difference in a case study using our proposed model for headway distances of 9 m and 12 m. The results are shown in Table 3 and Table 4.

Table 3. Coupled distribution (%) of velocity and velocity difference with headway distance of 9 m.

Velocity difference/(m/s)	Velocity/(m/s)															
	0	1	2	3	4	5	6	7	8	9	10	11	12	13	14	Sum
–6	–	0.12	–	–	–	–	–	–	–	–	–	–	–	–	–	0.12
–5	0.24	0.49	0.61	0.24	0.12	–	–	–	–	–	–	–	–	–	–	1.70
–4	0.12	0.61	1.46	0.85	2.19	0.24	–	–	–	–	–	–	–	–	–	5.47
–3	–	0.12	1.95	2.19	3.78	4.02	1.46	–	–	–	–	–	–	–	–	13.52
–2	–	0.24	–	0.85	2.07	5.36	10.72	1.10	–	–	–	–	–	–	–	20.34
–1	–	–	–	0.24	2.07	1.83	4.87	7.19	1.34	–	–	–	–	–	–	17.54
0	–	–	0.12	–	–	0.97	1.95	3.17	4.99	0.12	–	–	–	–	–	11.32
1	–	–	–	–	–	0.37	0.85	1.95	2.56	1.46	–	–	–	–	–	7.19
2	–	–	–	0.12	0.12	0.12	0.24	0.85	1.58	1.10	0.85	–	–	–	–	4.98
3	–	–	–	–	–	–	0.12	0.49	1.46	1.58	1.22	0.85	–	–	–	5.72
4	–	–	–	–	–	–	–	–	0.12	0.61	1.10	0.85	1.95	–	–	4.63
5	–	–	–	–	–	–	–	–	0.24	0.37	0.49	1.71	1.34	0.61	–	4.76
6	–	–	–	–	–	–	–	–	–	–	0.24	0.37	0.61	0.49	0.49	2.20
7	–	–	–	–	–	–	–	–	–	–	–	–	0.24	0.24	–	0.48
Sum	0.36	1.58	4.14	4.49	10.35	12.91	20.21	14.75	12.29	5.24	3.90	3.78	4.14	1.34	0.49	100

Table 4. Coupled distribution (%) of velocity and velocity difference with headway distance of 12 m.

Velocity difference/(m/s)	Velocity/(m/s)																
	0	1	2	3	4	5	6	7	8	9	10	11	12	13	14	15	Sum
–6	–	–	0.17	0.34	–	–	–	–	–	–	–	–	–	–	–	–	0.51
–5	0.17	0.17	0.17	0.34	0.69	0.34	–	–	–	–	–	–	–	–	–	–	1.88
–4	–	–	–	1.20	0.51	1.03	1.54	0.51	–	–	–	–	–	–	–	–	4.79
–3	–	–	–	0.17	1.20	1.20	2.06	3.95	1.54	0.34	–	–	–	–	–	–	10.46
–2	–	0.17	–	0.17	0.34	0.69	1.72	3.43	5.49	6.86	1.37	–	–	–	–	–	20.24
–1	–	–	–	–	0.17	0.17	0.17	0.69	4.63	6.17	9.78	0.34	–	–	–	–	22.12
0	–	–	–	–	–	0.34	0.17	0.34	1.37	1.72	2.57	3.09	–	–	–	–	9.58
1	–	–	–	–	–	0.17	–	0.34	0.51	0.86	1.72	2.06	0.51	–	–	–	6.17
2	–	–	–	–	–	–	0.17	0.34	0.86	0.34	0.86	1.72	0.34	0.34	–	–	4.97
3	–	–	–	–	–	–	–	–	–	0.17	0.86	0.51	2.06	0.51	0.69	–	4.80
4	–	–	–	–	–	–	–	–	–	–	0.86	1.72	1.03	2.06	1.20	0.51	7.38
5	–	–	–	–	–	–	–	–	–	–	–	0.17	0.69	0.17	2.06	0.86	3.95
6	–	–	–	–	–	–	–	–	–	–	–	–	0.17	0.17	1.03	1.20	5.354
7	–	–	–	–	–	–	–	–	–	–	–	–	–	–	–	0.17	0.17
8	–	–	–	–	–	–	–	–	–	–	–	–	–	0.17	0.17	–	0.34
Sum	0.17	0.34	0.34	2.22	2.91	3.94	5.83	9.60	14.40	16.46	18.02	9.61	4.80	3.42	5.15	2.74	100

Since, in the proposed model, $P_{\Delta v,9,6,a}$ and $P_{\Delta v,12,10,a}$ are the maximum values in the two groups $P_{\Delta v,9,j,a}$ $(j = 0,1,\ldots,14)$ and $P_{\Delta v,12,j,a}$ $(j = 0,1,\ldots,15)$ respectively, we chose state parameter groups $G_{\Delta v,9,6,a}$ and $G_{\Delta v,12,10,a}$ to be used as a contrast. The results are shown in Fig. 9.

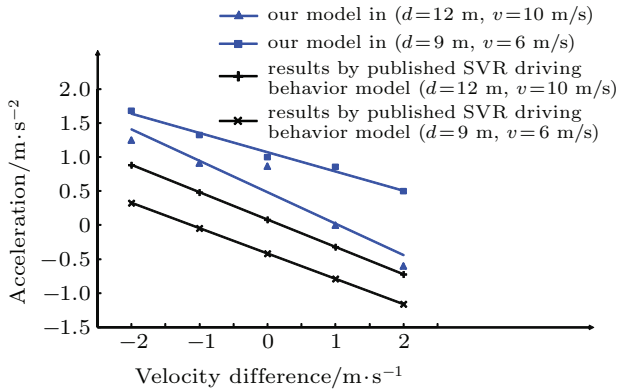


Fig. 9. The model comparison of the proposed model and the SVR driving behavior model.

The values of acceleration are a little higher than the results of the SVR driving behavior model, mainly because this model's acceleration strategy of allowing a driver to accelerate as long as there is a safe headway distance, is more radical than that of the SVR driving behavior model. The results also show that the proposed model reveals the law that acceleration has a linear correlation with the velocity difference when the absolute value of acceleration is not, in general, large. Thus, the results reflect the superiority of the proposed model, in that this model can present more detailed correlations between state parameters. The results indicate that the assumption that acceleration and deceleration rates can be considered to be constant in most empirical models, needs to be reevaluated.

5. Conclusion

In this paper, we describe and then analyze a new cellular automaton (CA) model designed to account for stochasticity in traffic flow induced by heterogeneity in driving behavior. The proposed model overcomes two major limitations of many of the published CA models for traffic modeling. One is the overdependence on directly changing a vehicle's velocity in the model's updating rules, and the other is the selection of a discrete constant value for acceleration which does not completely accord with reality. The proposed model also takes into account using safe distances to limit the value of acceleration to avoid collisions between vehicles. The model still uses discrete integer values for the state parameters of vehicles in the model simulation. As is well known, the calculation and execution time of a CA model is proportional to both the number of vehicles in the system and the number of iteration steps. The calculating and executing efficiency of the proposed model is $(3.18 \pm 0.05) \times 10^{-3}$ s/(veh·step) when the model runs on a computer with central processing unit (CPU) of Intel(R) Core(TM) i7-7700 HQ CPU@2.80 GHz and random access memory (RAM) of 16.0 GB. The high calculation and execution efficiency makes it possible to conduct real-time simulations of urban scale traffic scenarios based on this model.

Simulation results indicated that the new model is a highly capable model for modeling traffic flow whose performance is quite competitive from both macroscopic and microscopic perspectives. In particular, simulation results for a road segment with periodic boundary conditions indicated that the proposed model is capable of reproducing most empirical findings, including the fundamental diagram which depicts the three phases (free flow, synchronized flow, and jammed flow),

and the backward movement of a traffic jam in congested flow. This model also has a stronger ability to simulate free flow, light synchronized flow, and heavy synchronized flow at the same time.

This model can also take apart the detailed coupling correlation between a vehicle's different state parameters, which is difficult for other existing CA models. This model is capable of delineating the distributions of velocity with different headway distances, the correlation between the headway distance and the average velocity, and the correlation between velocity difference and acceleration of vehicles. The proposed CA model also shows that acceleration has a linear correlation with velocity difference when the absolute value of acceleration is not particularly large in general which is consistent with common findings in other models.

We plan to extend our proposed model in future to incorporate more realistic urban traffic systems, taking into consideration different types of vehicles and real-time updates of traffic conditions.

References

[1] Kerner B S and Konhäuser P 1994 *Phys. Rev. E* **50** 54
[2] Treiber M, Hennecke A and Helbing D 1999 *Phys. Rev. E* **59** 239
[3] Bando M, Hasebe K, Nakanishi K, Nakayama A, Shibata A and Sugiyama Y 1995 *J. Phys. I* (France) **5** 1389
[4] Nagel K and Schreckenberg M 1992 *J. Phys. I* (France) **2** 2221
[5] Adriana S M, Mirian B O, Mauricio C and Chen C 2002 *Int. J. Intell. Syst.* **17** 125
[6] Barceló J 2010 *Fundamentals of Traffic Simulation* (New York: Springer-Verlag)
[7] Liang J Y, Zhang L L, Luan X D, Guo J L, Lao S Y and Xie Y X 2017 *Acta Phys. Sin.* **66** 194501 (in Chinese)
[8] Krauss S, Wagner P and Gawron C 1997 *Phys. Rev. E* **55** 5597
[9] Barlovic R, Santen L, Schadschneider A and Schreckenberg M 1998 *Eur. Phys. J. B* **5** 793
[10] Kerner B S 1998 *Phys. Rev. Lett.* **81** 3797
[11] Kerner B S and Klenov S L 2003 *Phys. Rev. E* **68** 036130
[12] He S, Guan W and Song L 2010 *Physica A* **389** 825
[13] Xiang Z T, Li Y J, Chen Y F and Xiong L 2013 *Physica A* **392** 5399
[14] Xue Y, Jia L S, Teng W Z and Lu W Z 2015 *Commun. Nonlinear Sci.* **22** 285
[15] Jin C J, Wang W and Jiang R 2014 *Chin. Phys. B* **23** 024501
[16] Tian J, Jiang R, Jia B, Gao Z and Ma S 2016 *Transport. Res. B* **93** 338
[17] Jiang R and Wu Q S 2006 *Physic A* **364** 493
[18] Spyropoulou I 2007 *Transport. Res. C* **15** 175
[19] Meng Q and Weng Q J 2011 *Transport. Res. C* **19** 1263
[20] Zhu H J, Wang D and Zhou J B 2014 *Appl. Mech. Mater.* **587–589** 2213
[21] Khallouk A, Lakouari N, Echab H and Ez-Zahraouy H 2017 *Int. J. Mod. Phys. C* **28** 1750093
[22] Regragui Y and Moussa N 2018 *Chin. J. Phys.* **56** 1273
[23] Guzmán H A, Lárraga M E, Alvarez-Icaza L and Carvajal J 2018 *Physica A* **491** 528
[24] Guzmán H A, Lárraga M E, Alvarez-Icaza L and Huerta F 2014 *UKSim-AMSS 8th European Modelling Symposium*, October 21–23, 2014, Pisa, Italy, p. 126
[25] Hsu C C and Chiou Y C 2018 *J. Adv. Transport.* **8961454**
[26] Maleck K 2018 *J. Comput. Sci.* **28** 32
[27] Yang L H, Zhang X Q and Ji W C 2018 *Ksce J. Civ. Eng.* **22** 5187
[28] Lárraga M E and Alvarez-Icaza L 2010 *Physica A* **389** 5425
[29] Lee H K, Barlovic R, Schreckenberg M and Kim D 2004 *Phys. Rev. Lett.* **92** 238702
[30] Wang Y and Chen Y Y 2015 *Chin. Phys. B* **24** 038902
[31] Wei D L and Liu H C 2013 *Transport. Res. B* **47** 1
[32] Huang X L, Sun Jie and Sun Jian 2018 *Transport. Res. C* **95** 346
[33] Bareket Z, Fancher P S and Ervien R D 1998 Fostering Development, Evaluation, and Deployment of Forward Crash Avoidance Systems (FOCAS), Annual Research Report (University of Michigan, Transportation Research Institute ARRJ-15-95), Ann Arbor, MI
[34] Li X C, Luo X, He M C and Chen S W 2018 *Physica A* **509** 536
[35] Chen J X, Li Z B, Jiang H, Zhu S L and Wang W 2017 *Physica A* **468** 880
[36] Alvarez L and Horowitz R 1999 *Vehicle Syst. Dyn.* **32** 23
[37] Benjamin S C, Johnson N F and Hui P M 1996 *J. Phys. A* **29** 3119
[38] Mallikarjuna Ch and Ramachandra Rao K 2011 *Transportmetrica A* **7** 321
[39] Schadschneider A and Schreckenberg M 1997 *Ann. Phys.* (Berlin) **509** 541
[40] Knospe W, Santen L, Schadschneider A and Schreckenberg M 2000 *J. Phys. A* **33** L477
[41] Tomoeda A, Miyaji T and Ikeda K 2018 *Transportmetrica A* **14** 503
[42] Jiang R and Wu Q S 2003 *J. Phys. A* **36** 381
[43] Zhang Z Y, Rong J and Ren F T 2004 *J. Highway Transport. Res. Dev.* **8** 108 (in Chinese)
[44] Jin C J, Knoop V L, Jiang R, Wang W and Wang H 2018 *IET Intell. Transp. Syst.* **12** 359
[45] Jin C J, Wang W, Jiang R, Zhang H M, Wang H and Hu M B 2015 *Transport. Res. C* **60** 324
[46] Jin C J, Wang W, Jiang R, Zhang H M and Wang H 2013 *Phys. Rev. E* **87** 012815
[47] Jin C J, Wang W, Jiang R and Wang H 2014 *J. Phys. A: Math. Theor.* **47** 125104